

## PRIORITY COMMUNICATION

# Universality in Heterogeneous Catalysis

J. K. Nørskov,<sup>\*,1</sup> T. Bligaard,<sup>\*</sup> A. Logadottir,<sup>\*</sup> S. Bahn,<sup>\*</sup> L. B. Hansen,<sup>\*</sup> M. Bollinger,<sup>\*</sup> H. Bengaard,<sup>\*</sup>  
B. Hammer,<sup>†</sup> Z. Sljivancanin,<sup>†</sup> M. Mavrikakis,<sup>‡</sup> Y. Xu,<sup>‡</sup> S. Dahl,<sup>§</sup> and C. J. H. Jacobsen<sup>§</sup>

<sup>\*</sup>Center for Atomic-scale Materials Physics, Department of Physics, Building 307, Technical University of Denmark, DK-2800 Lyngby, Denmark; <sup>†</sup>Institute of Physics and Astronomy, University of Aarhus, DK-8000 Aarhus C, Denmark; <sup>‡</sup>Department of Chemical Engineering, University of Wisconsin-Madison, Madison, Wisconsin 53706; and <sup>§</sup>Haldor Topsøe A/S, Nymøllevej 55, DK-2800 Lyngby, Denmark

Received July 3, 2001; revised March 25, 2002; accepted March 25, 2002

Based on an extensive set of density functional theory calculations it is shown that for a class of catalytic reactions there is a universal, reactant independent relation between the reaction activation energy and the stability of reaction intermediates. This leads directly to a universal relationship between adsorption energies and catalytic activity, which is used to pinpoint what it is that determines the best catalyst for a given reaction. The universality principle rationalizes a number of known facts about catalysts and points to new ways of improving them. © 2002 Elsevier Science (USA)

The empirical knowledge of catalysis and catalysts is enormous (1). We know, for instance, that Pd and Pt–Rh are the best exhaust catalysts for NO removal (2), while Co, Fe, and Ru are the best Fischer–Tropsch catalysts (3), Pt, Pd, and Ag are the best oxidation catalysts (4), and Ru and Fe are the best ammonia synthesis catalysts (5). But in general we do not know why. In the present communication we show that for a class of reactions proceeding over transition metal catalyst surfaces, there is a universal, reaction-independent relationship between activation energies and the stability of important intermediates in the reaction. On this basis we can understand semiquantitatively what it is that characterizes the optimum catalyst for all the reactions belonging to the class.

The reactions we will focus on here can be characterized as “activation of a diatomic molecule.” Ammonia synthesis ( $\text{N}_2 + 3\text{H}_2 \rightarrow 2\text{NH}_3$ ) is, for instance, activation of  $\text{N}_2$  in the sense that  $\text{N}_2$  is first dissociated, whereafter the dissociation products are hydrogenated into the final product. Hydrogen also needs to dissociate, but this reaction is fast and hydrogen binds more weakly to the surface than nitrogen. For this reason the  $\text{N}_2$  activation is the key aspect of the reaction. Similarly, Fischer–Tropsch synthesis (e.g.,  $n\text{CO} + (2n + 1)\text{H}_2 \rightarrow \text{C}_n\text{H}_{2n+2} + n\text{H}_2\text{O}$ ) can be char-

acterized as CO activation, NO reduction in a car exhaust system as NO activation, and some oxidation reactions as  $\text{O}_2$  activation.

All these reactions have two main parts: The dissociation of the reacting molecules and the removal of the dissociation products. The rate of dissociation is determined by the activation barrier for dissociation,  $E_a$ , while the rate of product removal is given largely by the stability,  $\Delta E$ , of the intermediates on the surface; see Fig. 1. A good catalyst is characterized by a low activation energy *and* weak bonding of the intermediates. It has long been realized that  $E_a$  and  $\Delta E$  are often correlated such that the best catalyst is a compromise having adsorbate–surface interactions of intermediate strength. This is also known as the Sabatier principle (6, 7). The first step toward placing such qualitative considerations on a more firm basis was taken recently, when it was shown that there is indeed a direct, linear relationship between  $E_a$  and  $\Delta E$ . Using density functional theory (DFT) calculations to treat the same process on different transition metal surfaces, such a relationship has been shown to exist for CH bond breaking by Pallassana and Neurock (8), for CO dissociation by Liu and Hu (9), and for  $\text{N}_2$  dissociation by Logadottir *et al.* (10).

Focusing first on the results for  $\text{N}_2$  activation, there is a clear, linear Brønsted–Evans–Polanyi-type (11, 12) relationship between the activation energy for dissociation and the nitrogen–surface bond energy; cf. Fig. 2. In fact there are several such relationships, depending on the surface structure. Figure 2 includes one for close-packed surfaces and another for special step sites where five metal atoms can be used for dissociation (10). Clearly, the step-type sites are most reactive. This has also been shown experimentally in several cases (13–15). When combined with a kinetic model for ammonia synthesis, the linear relationship between activation energy and nitrogen–surface bond energy translates into a volcano-shaped dependence of the catalytic activity on the nitrogen adsorption energy; see Fig. 2c (10).

<sup>1</sup> To whom correspondence should be addressed. E-mail: norskov@fysik.dtu.dk.

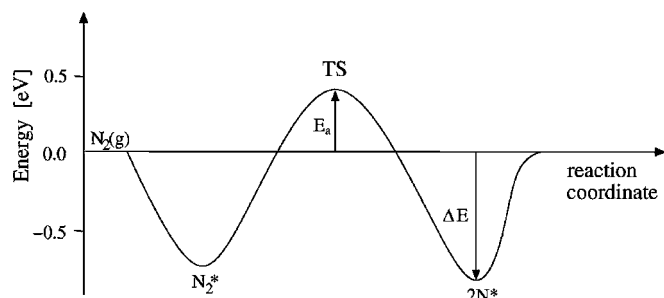


FIG. 1. Calculated potential energy diagram for  $N_2$  activation at a Ru step. The molecularly ( $N_2^*$ ) and atomically adsorbed ( $N^*$ ) states, as well as the transition state for dissociation (TS), are indicated. The rate of dissociative adsorption is given by the transition state energy,  $E_a$ , while the stability of the dissociated product is given by the chemisorption energy,  $\Delta E$ .

We now include data for CO, NO, and  $O_2$  dissociation on a number of different metals; see Table 1. A total of 84 transition and final states have been located on the basis of periodic slab density functional theory calculations utilizing ultrasoft pseudopotentials, a plane wave basis set with a cutoff of 25 Ry, and the GGA–RPBE description of exchange and correlation (16). The calculational procedure is outlined in detail in Ref. (10).

The unexpected finding is that all results fall on the same Brønsted–Evans–Polanyi lines in Fig. 2. This means that within the accuracy of the DFT calculations there is a universal relation for all the molecules studied here. Knowledge of the adsorption energy of the intermediates, either from experiments or from calculations, can therefore be used to estimate the activation energies using the linear relationships  $E_a = (2.07 \pm .07) + \Delta E \cdot (0.90 \pm .04)$  (close-packed surfaces, Fig. 2a) and  $E_a = (1.34 \pm .09) + \Delta E \cdot (0.87 \pm .05)$  (steps, Fig. 2b), all energies in eV.

The existence of a universal Brønsted–Evans–Polanyi line immediately raises three questions: Why is the relationship between  $E_a$  and  $\Delta E$  linear? Why is it structure-dependent? And why is it adsorbate-independent? The answer to all three questions lies in the nature of the transition state structures. It turns out that for a given metal surface geometry, the transition state structures are essentially independent of the molecule and the metal considered; see Fig. 3 (18). In addition, the bond length in the transition state is quite long, and the constituent atoms have largely lost their molecular identity. This means that variations in the transition state energy will follow that of the final state energy closely giving a linear relationship with a slope close to one. Since the transition state structures do depend on the local surface structure, the Brønsted–Evans–Polanyi lines are different for different sites on the surface. Finally, the fact that the transition state geometries are so similar for different reactants is the reason that the relationship is adsorbate-independent.

The universality of the Brønsted–Evans–Polanyi curve for the class of molecules considered here has an interest-

ing consequence. If we assume that the overall kinetics of these reactions follows the same pattern—dissociation is rate limiting when the barrier is high and blocking of the surface is limiting the reactivity when the adsorbates bind strongly to the surface—then the universality in Fig. 2 translates into universality in terms of the volcano curves. If we take the ammonia kinetics as a guideline, the optimum catalyst should be one with an adsorbate binding energy in the range  $-1.4$ – $-0.8$  eV ( $-140$ – $-80$  kJ/mole); cf. Fig. 2c. For ammonia synthesis ( $N_2$  activation) both Ru and Fe lie within this range; see Table 1. For CO activation (Fischer–Tropsch synthesis) the same is true for Rh, Co, Ni, and Ru, and for NO activation it is Pd and Pt. For  $O_2$  activation none of the metals we have considered are in

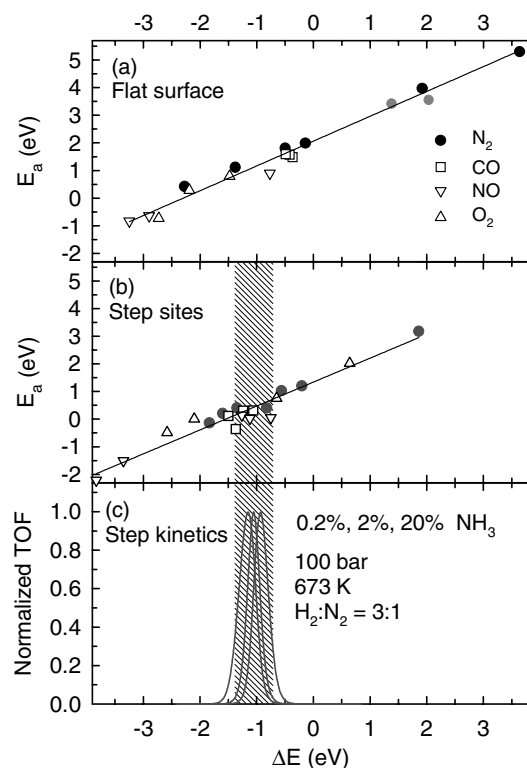


FIG. 2. Calculated activation energies ( $E_a$ ; see Fig. 1) for  $N_2$ , CO, NO, and  $O_2$  dissociation on a number of different metals plotted as a function of the calculated dissociative chemisorption potential energy for the dissociation products ( $\Delta E$ ; see Fig. 1). The data are shown in Table 1. Results for close packed surfaces (fcc(111), hcp(0001), and bcc(110)) (a) as well as for steps (which include fivefold coordinated sites) (b) are included. They show the same trends, but group along two different straight lines. The steps are more reactive than the terraces for these reaction and will tend to dominate the reactivity unless poisoned in some way. For  $N_2$ /Ru(0001) we also include data for a high coverages (0.5 monolayers) of oxygen and nitrogen (gray points). The linear relationship for  $N_2$  dissociation on the most reactive step sites (red points in (b)) has been used as input into a kinetic model for the ammonia synthesis reaction (10). The calculated reactivity per site per second (the turnover frequency, TOF) normalized to give the same maximum value is shown for different reaction conditions (c). The optimum reactivity depends somewhat on reaction conditions and occurs for an adsorbate–surface interaction energy in the range  $-1.4$  to  $-0.8$  eV.

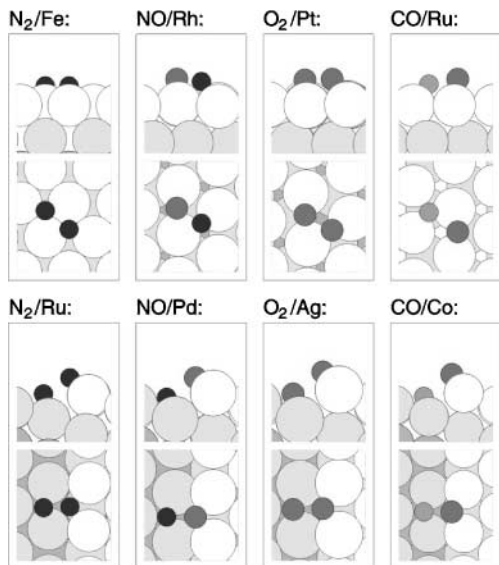


FIG. 3. Calculated transition state structures for  $N_2$ , NO, CO, and  $O_2$  dissociation on different transition metal surfaces. Results for close-packed surfaces are shown in the upper row and for stepped surfaces in the lower row. N is shown blue, O red, and C gray.

the optimum range, but the closest are Ag ( $-0.65\text{eV}$ ), Pd ( $-1.56\text{eV}$ ), and Pt ( $-2.2\text{eV}$ ). The agreement of this simple principle with empirical observations is remarkable.

The important parameter characterizing the reactivity of a given metal is the adsorbate surface interaction energy,  $\Delta E$ , in the final state of the dissociation process. This parameter has its optimum value for different metals depending on the nature of the reactants, and the variation in optimum catalyst from one reaction to the next follows directly from this principle. We note that it is only with access to the large database of the DFT calculations that we can now establish such a principle and test it.

The present treatment is only aimed at understanding the overall trends in the catalytic activity. There are several reasons for this. First of all, we do not treat the reaction steps following activation of the main reactant molecule in any detail. Including these may change the kinetics somewhat. This will be less of a problem, when the other reactants are easy to activate. Reactions with hydrogen or CO (nondissociated) should belong to this class. Oxidation reactions where  $O_2$  reacts with saturated hydrocarbons, on the other hand, may not belong to the class. In this case the hydrocarbon activation can also be decisive. We

TABLE 1

Calculated (DFT-RPBE) Adsorption Energies ( $\Delta E$ ) and Transition State Energies ( $E_a$ ) in eV, Relative to the Free Molecule

	$N_2$		CO		NO		$O_2$	
	$\Delta E$	$E_a$	$\Delta E$	$E_a$	$\Delta E$	$E_a$	$\Delta E$	$E_a$
Mo(110)	-2.27	0.42						
Mo-step	-1.83	-0.14						
Fe(110)	-1.38	1.11						
Fe-step	-1.35	0.40						
Ru(0001)	-0.50	1.80	-0.49*	1.59*	-3.25*	-0.83*	-4.53	
Ru-step	-0.82	0.40	-1.37*	-0.36*	-3.83*	-2.21*	-4.98*	
Co-step	-0.20	1.20	-1.24	0.31				
Co-Mo-step I	-1.60	0.20						
Co-Mo-step II	-1.28	0.25						
Rh(111)	-0.14	1.99	-0.37	1.48	-2.90	-0.64	-3.76	
Rh-step	-0.56	1.03	-1.06	0.32	-3.35	-1.50	-4.24	
Ir(111)							-2.80	-0.73
Ni(111)			-0.42	1.58			-3.96	
Ni-step			-1.50	0.11				
Pd(111)	1.92	3.97		2.70	-0.77	0.90	-1.54	
Pd-step	1.86	3.17		1.79	-0.75	0.05	-1.56	
Pt(111)							-1.48	0.80
Pt-step					-1.26	0.14	-2.10	0.00
Pt/Rh-step					-1.12	0.26		
Cu(111)	3.64*	5.30*					-2.19	0.29
Cu-step							-2.58	-0.49
Ag(111)							-0.29	1.50
Ag-step							-0.65	0.75
Au(111)							0.86	
Au-step							0.54	1.33

Note. The two energies are defined in Fig. 1. In most cases both values are calculated and used as input into Fig. 2, but some cases where only the adsorption energy is calculated are included. In most cases both adsorbate and metal coordinates have been optimized, but for systems marked with a \* only the adsorbate degrees of freedom have been relaxed. Co-Mo-step I and II refer to Mo- and Co-rich sites, respectively, on the same 50-50 alloy, while Pt/Rh step refers to Pt with Rh in the second layer.

also note that we are not treating questions relating to selectivity here.

Another limitation is that the accuracy of the DFT calculations is not such that we can give a quantitative treatment. There are also deviations from the linear behavior in Fig. 2. We are neglecting them in the present overall treatment, but these deviations may well turn out to be essential in the last fine-tuning of the reactivity of a given system.

Reactions with transition states that are different from those considered here may also show linear Brønsted–Evans–Polanyi relations, but not necessarily the same. This is true for CH activation (8), for H<sub>2</sub> activation, and for H<sub>2</sub>O activation, for example. Such reactions will belong to different classes of reactions with optimum interaction strengths different from the one found here for the class of reactions involving medium-size diatomics. The general principles may therefore be applicable to other classes of reactions.

We have concentrated here on differences between different metals and have not explicitly treated the effect of adsorbate–adsorbate interactions. This can easily be incorporated, though. In Fig. 2a we have included some points for N<sub>2</sub> activation on Ru(0001) in the presence of high coverages of nitrogen or oxygen (18). They are merely shifted to (much) weaker bonding, but are still close to the Brønsted–Evans–Polanyi line. It means that if the reaction conditions are changed such that the coverage of an intermediate changes significantly then adsorbate–adsorbate interactions may effectively shift the corresponding point to another position along the line. An example of such an effect may be provided by the recent work of Over *et al.* on CO oxidation over RuO<sub>2</sub> (19). Ru is a poor oxidation catalyst. It binds oxygen much too strongly; cf. Table 1. But if the reaction conditions are such that RuO<sub>2</sub> is formed, then a new much weaker bound state of adsorbed oxygen appears (thermal desorption experiments suggests an adsorption energy of about  $-1.2$  eV (20) and DFT calculations a binding energy of  $-1.05$  eV (21)), and the oxide is catalytically very active (19, 20).

The universal relation between activation energy and binding energy directly suggests a general approach to optimizing the catalyst by searching for new materials with adsorbate–surface interaction strengths in the right range. This principle has already been used to find a new ammonia catalyst (22). The adsorption properties of N<sub>2</sub> on CoMo alloys turn out to be intermediate between those of Co and Mo which bind nitrogen either too weakly or too strongly; cf. Table 1. The alloy has adsorption properties close to op-

timum (cf. Table 1) and it has been found experimentally to be a much better ammonia catalyst than either constituent (22). There is therefore good reason to expect that the same principle of looking for surfaces with close to optimum adsorption strengths can be applied to find better catalysts for the other reactions in this class as well as in other classes of reactions.

## ACKNOWLEDGMENTS

The Center for Atomic-Scale Materials Physics is sponsored by the Danish National Research Foundation. MM acknowledges partial financial support from an NSF-CAREER award (CTS-0134561).

## REFERENCES

1. Ertl, G., Knözinger, H., and Weitkamp, J., Eds., "Handbook of Heterogeneous Catalysis," Wiley–VCH, Weinheim, 1997.
2. Nieuwenhuys, B. E., *Surf. Rev. Lett.* **50**, 1869 (1996).
3. Vannice, M. A., *J. Catal.* **50**, 228 (1977).
4. Muhler, M., in "Handbook of Heterogeneous Catalysis" (G. Ertl, H. Knözinger, and J. Weitkamp, Eds.), Vol. 5, p. 2274. Wiley–VCH, Weinheim, 1997.
5. Topsøe, H., Boudart, M., and Nørskov, J. K., Eds., "Frontiers in Catalysis: Ammonia Synthesis and Beyond." *Top. Catal.* **1** (1994).
6. Sabatier, P., "La catalyse en chimie organique." Béranger, Paris, 1920.
7. Balandin, A. A., *Adv. Catal.* **19**, 1 (1969).
8. Pallassana, V., and Neurock, M., *J. Catal.* **191**, 301 (2000).
9. Liu, Z.-P., and Hu, P., *J. Chem. Phys.* **114**, 8244 (2001).
10. Logadottir, A., Rod, T. H., Nørskov, J. K., Hammer, B., Dahl, S., and Jacobsen, C. J. H., *J. Catal.* **197**, 229 (2001).
11. Brønsted, N., *Chem. Rev.* **5**, 231 (1928).
12. Evans, M. G., and Polanyi, N. P., *Trans. Faraday Soc.* **34**, 11 (1938).
13. Zambelli, T., Wintterlin, J., Trost, J., and Ertl, G., *Science* **273**, 1688 (1996).
14. Dahl, S., Logadottir, A., Egeberg, R. C., Larsen, J. H., Chorkendorff, I., Törnqvist, E., and Nørskov, J. K., *Phys. Rev. Lett.* **83**, 1814 (1999).
15. Gambardella, P., Slijvančanin, Z., Hammer, B., Blanc, M., Kuhnke, K., and Kern, K., *Phys. Rev. Lett.* **87**, 056103 (2001).
16. Hammer, B., Hansen, L. B., and Nørskov, J. K., *Phys. Rev. B* **59**, 7413 (1999).
17. The only exception is the O<sub>2</sub>/Pt step where it is parallel to the step.
18. Hammer, B., *Phys. Rev. B* **63**, 205423 (2001).
19. Over, H., Kim, Y., Seitsonen, A. P., Wendt, S., Lundgren, Shmid, M., Varga, P., Morgante, A., and Ertl, G., *Science* **287**, 1474 (2001).
20. Kim, Y., Seitsonen, A. P., Wendt, S., Wang, J., Fan, C., Joci, K., Over, H., and Ertl, G., *J. Phys. Chem. B* **105**, 3752 (2001).
21. Reuter, K., and Scheffler, M., *Phys. Rev. B* **65**, 035406 (2002).
22. Jacobsen, C. J. H., Dahl, S., Clausen, B. S., Bahn, S., Logadottir, A., and Nørskov, J. K., *J. Am. Chem. Soc.* **123**, 8404 (2001).